scientific reports

Check for updates

OPEN

Exploring cortical excitability in children with cerebral palsy through lower limb robot training based on MI-BCI

Weihang Qi[1,5], Yi Zhang[1,5], Yuwei Su[1], Zhichong Hui[1], ShaoQing Li[1], HaoChong Wang[3], Jiamei Zhang[1], Kaili Shi[1], Mingmei Wang[1], Liang Zhou[4] & Dengna Zhu[1,2]✉

This study aims to compare brain activity differences under the motor imagery-brain-computer interface (MI-BCI), motor imagery (MI), and resting (REST) paradigms through EEG microstate and functional connectivity (FC) analysis, providing a theoretical basis for applying MI-BCI in the rehabilitation of children with cerebral palsy (CP). This study included 30 subjects aged 4–6 years with GMFCS II-III grade, diagnosed with CP and classified as spastic diplegia. They sequentially completed EEG signal acquisition under REST, MI, and MI-BCI conditions. Clustering analysis was used to analyze EEG microstates and extract EEG microstate temporal parameters. Additionally, the strength of brain FC in different frequency bands was analyzed to compare the differences under various conditions. Four microstate classes (A-D) were identified to best explain the datasets of three groups. Compared to REST, the average duration and coverage rate of microstate D under MI and MI-BCI significantly increased ($P < 0.05$), while their frequency and the coverage rate and frequency of microstate A decreased. Compared to MI, the average duration of microstate C under MI-BCI significantly decreased ($P < 0.05$), while the frequency of microstate B significantly increased ($P < 0.05$). Additionally, the transition probability results showed that other microstates under REST had a higher transition probability to microstate A, while under MI and MI-BCI, other microstates had a higher transition probability to microstate D. The brain network results revealed significant differences in brain network connectivity among REST, MI, and MI-BCI across different frequency bands. No FC differences were found between REST, MI, and MI-BCI in the α2 frequency band. In the δ and γ frequency bands, MI and MI-BCI both had greater inter-electrode connectivity strength than REST. In the θ frequency band, REST had greater inter-electrode connectivity strength than MI-BCI, while MI-BCI had greater inter-electrode connectivity strength than both REST and MI. In the α1 frequency band, MI-BCI had greater inter-electrode connectivity strength than REST, and in the β frequency band, MI-BCI had greater inter-electrode connectivity strength than MI. MI-BCI can significantly alter the brain activity patterns of children with CP, particularly by enhancing the activity intensity of EEG microstates related to attention, motor planning, and execution, as well as the brain FC strength in different frequency bands. It holds high application value in the lower limb motor rehabilitation of children with CP.

Keywords Cerebral palsy, MI-BCI, Cortical excitability, EEG microstate, Functional connectivity

Cerebral palsy (CP) is the most common disabling disease in childhood, typically caused by damage to the developing brain before, during, or after birth[1]. Epidemiological studies indicate that the incidence of CP is 2–3 per thousand, a rate that has remained relatively stable over the past few decades[2]. The rehabilitation treatment of children with CP is a complex and long-term process, characterized by continuous advancements in both traditional treatment methods and emerging therapeutic technologies. In recent years, significant progress has

[1]Department of Rehabilitation Medicine, The Third Affiliated Hospital of Zhengzhou University, Zhengzhou 450052, China. [2]Key Laboratory of Pediatrics Brain Injury in Henan Province, Henan Provincial Pediatrics Clinical Medical Research Centre, The Third Affiliated Hospital of Zhengzhou University, Zhengzhou 450052, China. [3]Institute of Health and Rehabilitation Science, School of Life Science and Technology, Xi'an Jiaotong University, Xi'an 710049, China. [4]Department of Imaging, The Third Affiliated Hospital of Zhengzhou University, Zhengzhou 450052, China. [5]Weihang Qi and Yi Zhang contributed equally. ✉email: zhudengna@126.com

been made in research on neuroregulation, robot-assisted devices, virtual reality technology, motor imagery (MI), and brain-computer interface (BCI) technology[3,4]. Among these, the combined application of MI and BCI, as an innovative rehabilitation approach, connects the neural signals of motor imagery from the brain with external devices, enabling conscious control and motor recovery in patients. This combined approach has garnered significant attention in the field of CP rehabilitation[5].

Motor imagery (MI) refers to simulating real movements in the brain, thereby generating specific neural signals in the motor cortex, such as changes in electroencephalogram (EEG) and blood flow information[6]. Research indicates that among various BCI paradigms, MI has drawn considerable attention for its ability to enhance motor function in patients with motor impairments[7]. Recently, a novel MI paradigm based on the concept of a "sixth finger" (SF-MI) has been introduced for stroke patients. Compared to traditional MI paradigms, this new approach exhibits enhanced the event-related desynchronization (ERD) patterns, with more synchronized and cohesive neural activity across different brain regions[8]. Studies have shown that children with hemiplegia can perform MI tasks[9]. For children, MI can serve as a reliable supportive or supplementary (at-home) rehabilitation tool for pediatric neurorehabilitation[10]. Imagery training may effectively, and even significantly, aid in enhancing or restoring motor networks within the pediatric nervous system under certain pathological conditions. Furthermore, numerous studies have indicated that the cortical activation patterns during actual movement and MI are very similar[11,12]. MI can activate brain regions involved in motor control, including the premotor cortex, supplementary motor area, parietal cortex, cingulate gyrus, basal ganglia, and cerebellum[13]. MI training for children with hemiplegia has demonstrated that MI can be effectively incorporated into the rehabilitation process[14]. BCI is a technology that directly acquires brain signals and converts them into computer commands to control external devices. The working principle of BCI is divided into four parts: signal acquisition, signal processing, device control, and feedback. This technology enables the brain to directly communicate with computers or other electronic devices without relying on other parts of the body, such as hands or voice.

The application prospects of MI-BCI in rehabilitation are broad. Neural information collection devices are used to gather the neural signals of subjects and identify motor intentions. These signals are then converted into computer commands that drive limb movement through a lower limb rehabilitation robot, forming a closed-loop feedback system. Meanwhile, MI relies on the mental simulation of actions, linking the brain's motor representations with the actual physical movement, which aids in the rehabilitation of motor functions[15,16]. BCI-based training aims to strengthen sensorimotor pathways by promoting motor learning and neuroplasticity[17]. It has been effectively applied to motor rehabilitation in patients with neurological disorders, particularly stroke patients[18]. Studies using functional MRI (fMRI) and navigated transcranial magnetic stimulation to assess the activity and excitability of the cortical motor area have shown that adding BCI to MI training can significantly enhance the excitability of the motor cortex in subjects, including the neurorehabilitation of CP patients[19]. Behboodi et al. developed and evaluated a BCI-based neurofeedback system that uses real-time EEG monitoring to support motor rehabilitation in children with CP[20]. The results showed that after 10 training sessions, patients experienced improvements in ankle dorsiflexion speed, walking speed, and stride length. Although MI-BCI has achieved certain results in adult rehabilitation, its application in the rehabilitation of children with CP is still limited. Existing studies have demonstrated that MI-BCI has potential application value in the motor rehabilitation of children with CP, significantly improving the brain's efficiency in processing motor-related information. This improvement is mainly achieved by promoting the effective redistribution of brain resources and enhancing inter-regional brain activity during the MI-BCI process[21]. However, further in-depth research is needed to verify the efficacy of MI-BCI in the daily rehabilitation training of children with CP and to explore the underlying neuroactivity mechanisms.

EEG microstates are transient representations of the brain's global functional state, related to widespread neural synchronous activity. Lehmann et al. used the k-means clustering method and cross-validation criteria to determine that the optimal number of EEG microstate types is four, and sequentially labeled these EEG microstates as types A (MS A), B (MS B), C (MS C), and D (MS D)[22]. In EEG activity, each microstate persists for a very short period (tens of milliseconds) and then rapidly transitions to another, maintaining its form within this brief timeframe. The study of EEG data can thus be intuitively simplified to the time series of these alternating scalp potential distributions[23]. Related research has also included microstate analysis under task conditions, such as studies on motor functions, auditory stimuli, visual stimuli, and driver brain load during driving tasks[24,25]. BCI can be controlled by CP patients[26]. Previous studies have conducted microstate analysis on MI-BCI, demonstrating the ability of microstate parameters as classification features[27,28], which help improve the classification accuracy of BCI systems and optimize their design. Additionally, some research has shown that during MI-BCI, healthy individuals and patients with paraplegia or quadriplegia exhibit different frequencies of microstate category occurrences, while no significant difference was found between paraplegic and quadriplegic patients[29].EEG functional connectivity (FC) refers to the detection of synchronized activity patterns between different brain regions within a specific time period, as measured by EEG technology. It reflects the dynamic processes of information transmission and communication between various brain regions and is a crucial approach to understanding brain functional organization. FC can be assessed by calculating metrics such as correlation, coherence, or phase synchronization between EEG signals. Studies have shown that FC exhibits significant changes during cognitive processes, emotion regulation, and in pathological states. For example, FC patterns in patients with Alzheimer's disease and depression differ significantly from those in healthy individuals[30,31]. Additionally, in stroke patients during the recovery process, there was a significant increase in regional centrality in the ipsilateral primary motor cortex and contralateral cerebellum, while regional centrality in the ipsilateral cerebellum decreased. Over time, the FC with these brain regions showed consistent changes[32]. Analyzing these connectivity patterns can provide important references for the diagnosis and treatment of neurological diseases. Research on FC is rapidly evolving, revealing the brain's complex network structures and

information processing mechanisms. Therefore, EEG microstate and FC analysis are promising cost-effective and clinically applicable neurophysiological methods for studying and evaluating the brain's overall functional state under healthy and diseased conditions.

Based on the above, this study aims to explore whether there are differences in brain activity under MI-BCI compared to MI and resting states, and what those differences are. By utilizing the rich temporal and spatial variation information from EEG microstate and FC analysis methods, we aim to provide a theoretical basis for the clinical rehabilitation application of MI-BCI in children with CP. In this study, we hypothesize that MI-BCI can significantly alter EEG microstate activity and improve the strength of FC across different frequency bands in children with CP. We believe this will provide a theoretical basis for rehabilitation training in these children and offer new insights for research in this field.

Materials and methods

This study was conducted in accordance with the World Medical Association Declaration of Helsinki and was approved by the Ethics Committee of the Third Affiliated Hospital of Zhengzhou University (Approval No.: 2023 - 184- 01) and registered at the Chinese Clinical Trial Registry (ChiCTR2400080145). Before the study, the researchers fully informed the legal representatives of each patient about the study protocol and obtained their informed consent.

General information

30 children with GMFCS II-III CP, aged 4–6 years, were recruited from the Department of Rehabilitation Medicine at the Third Affiliated Hospital of Zhengzhou University between February 1, 2024, and June 1, 2024. All participants were right-handed, as confirmed by the Edinburgh Handedness Inventory. Four children were unable to complete the pre-experiment, and the EEG data collected from six other children did not meet the requirements. A total of 20 children completed this experiment and provided good-quality EEG data, including 10 male and 10 female participants.

Inclusion criteria: ① Diagnosed with CP and classified as GMFCS II-III; ② Classified as spastic diplegia; ③ Have normal cognitive ability and are able to understand instructions and cooperate in completing training; ④ Able to reliably report pain, fear, and discomfort; ⑤ No orthopedic surgery or botulinum toxin treatment in the past 6 months; ⑥ Fully understand the trial content, voluntarily participate in the trial, with written informed consent signed by the subject's guardian.

Exclusion criteria: ① Severe lower limb contracture; ② Presence of complications involving important organs such as the heart, lungs, liver, or kidneys; ③ Accompanied by severe epilepsy, genetic metabolic diseases, and severe skeletal system diseases; ④ Presence of visual, auditory, or intellectual disabilities; ⑤ Have not undergone orthopedic surgery or botulinum toxin treatment in the past 6 months; ⑥ Participation in other lower limb rehabilitation clinical trials within 1 month before randomization in this study; ⑦ Children planning or expected to use new antispasmodic drugs, surgery, or other treatments during this study.

Experimental equipment

The experimental equipment is divided into two main parts: the BCI control system (see Fig. 1A) and the lower limb rehabilitation robot (see Fig. 1B).

The BCI control system includes an EEG signal acquisition system and a signal processing and classification system (ZhenTecBCI Co., Ltd., Xi'an, China). The EEG signal acquisition system includes an EEG cap, an EEG amplifier, and a data receiver. The EEG cap is equipped with electrodes placed according to the International 10–10 System, with 30 recording electrodes and two electrooculography electrodes (HEOR and HEOL), as shown in Fig. 2. The reference electrode is positioned at CPz, and the ground electrode is at Fz. All EEG electrodes, including the reference and ground electrodes, are Ag/AgCl semi-dry electrodes based on highly absorbent porous sponges soaked with 3% sodium chloride solution. The acquisition impedance is less than or equal to 20 kΩ, with a notch filter at 50 Hz and a sampling frequency of 500 Hz. The signal processing and classification system identifies whether the EEG signal activity intensity during MI exceeds the activation threshold. It then classifies the signals using intrinsic algorithms to send control commands to the lower limb rehabilitation robot, initiating movement. For detailed information on BCI classification algorithms, please refer to this paper[33].

The lower limb rehabilitation robot is a rigid device designed for children, developed by RoboCT Co., Ltd., Hangzhou, China. The equipment mainly consists of a control system, drive motors, and a mobile platform. The control system is responsible for generating gait movements, coordinating synchronous actions among the four actuators, and adjusting their movement parameters in real time based on state information such as the angular velocity of the motor shafts. The mobile platform has handrails at the rear and four wheels at the bottom, making it easy to move the equipment. Moreover, the equipment connects to the wearer's limbs via straps on the waist, thighs, calves, and feet. The distance between the two movable connecting segments of the waist support device can be adjusted with a width knob, making it suitable for subjects with different waist widths. Furthermore, during lower limb movements, the hydraulic system can move the waist support device vertically relative to the predetermined position.

Experimental procedure

Pre-experimental stage

The first objective of the pre-experiment is to use the signal processing and classification system to determine, for each subject, the EEG amplitude threshold that allows activation of the lower limb rehabilitation robot through MI. To determine the threshold, the subject wears the EEG equipment and stands still for 1 min, then continuously lifts their legs while standing for another 1 min. During this process, the signal processing and classification system automatically detects changes in EEG signal amplitude in the motor cortex during rest and

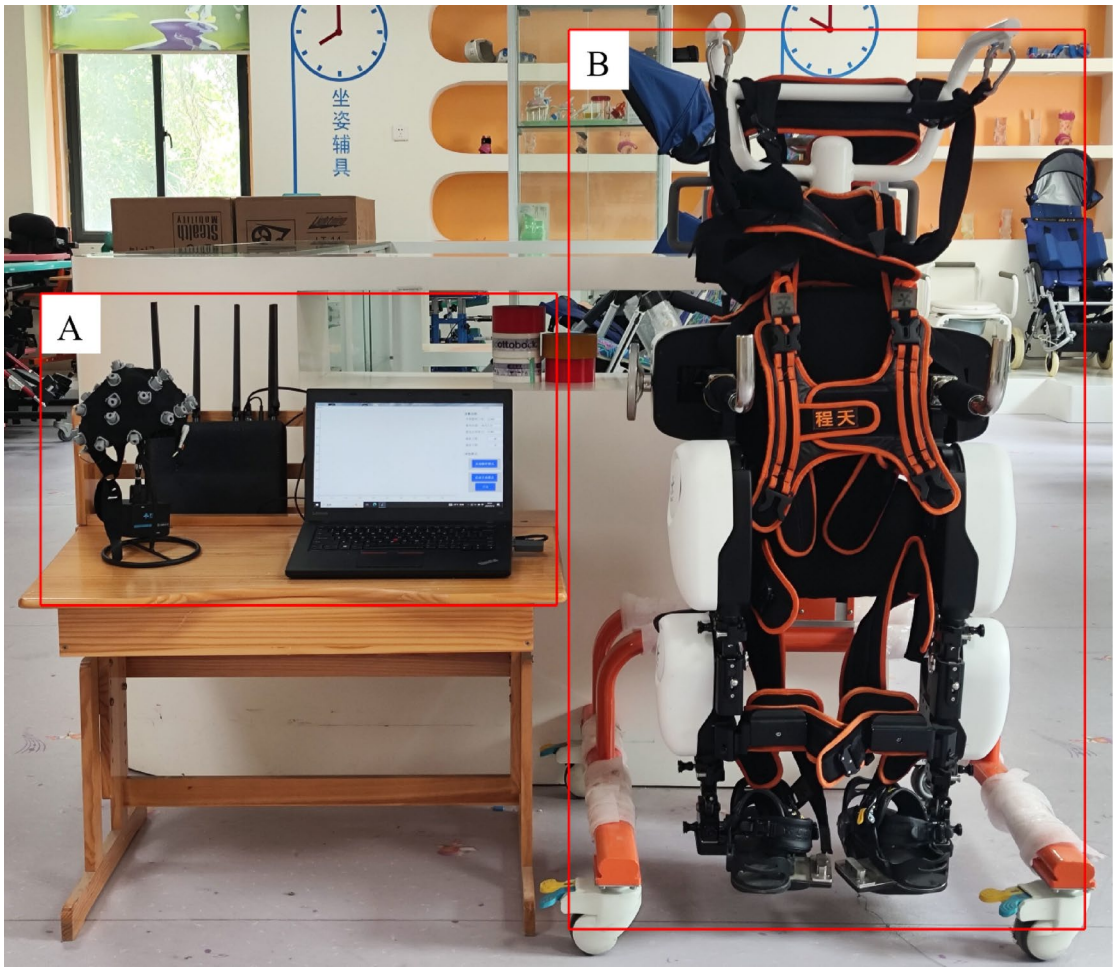

Fig. 1. (**A**) BCI control system; (**B**) Lower limb rehabilitation robot equipment.

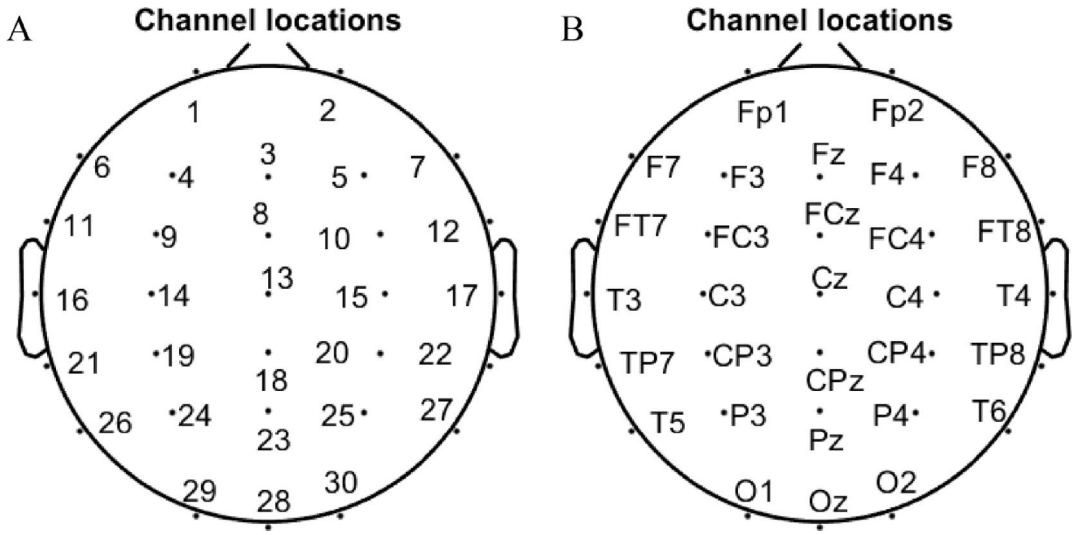

Fig. 2. Electrode Placement Diagram; (**A**) Number; (**B**) Name.

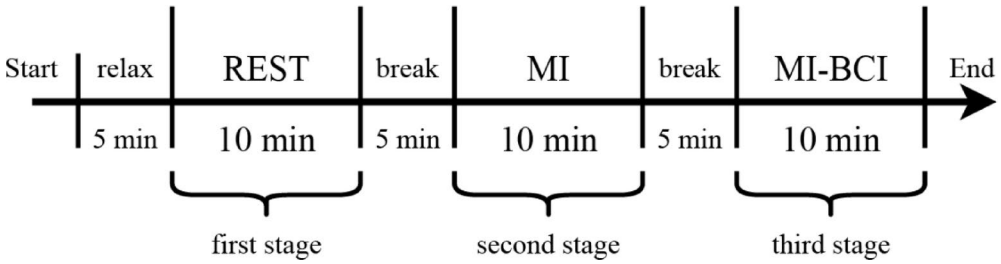

Fig. 3. Experimental Procedure.

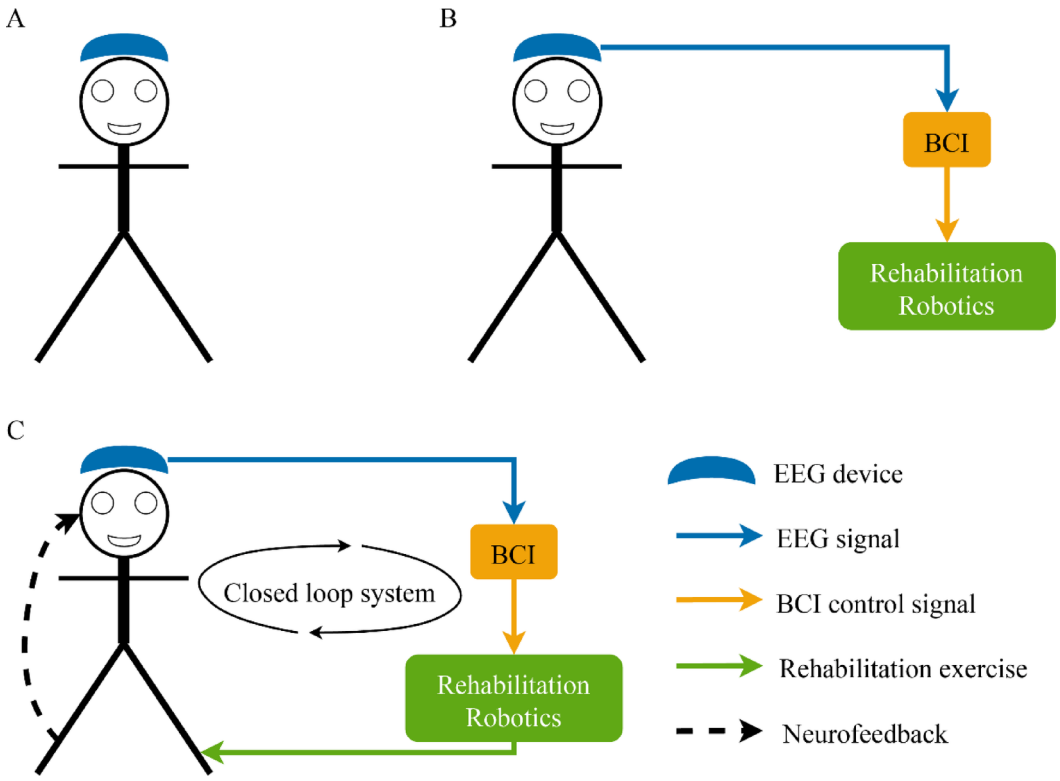

Fig. 4. Logical principle diagram; (**A**) REST; (**B**) MI; (**C**) MI-BCI.

during lower limb movement. This data is used to determine the threshold. After determining the threshold, the subject performs MI, and if it successfully activates the lower limb rehabilitation robot, the threshold is considered effective.

The second objective is to have the subjects undergo the complete experimental procedure during the pre-experiment stage, to familiarize themselves with the experimental equipment and environment. The experimental procedure is shown in Fig. 3.

Each subject undergoes the complete experimental procedure, which involves quietly resting in an undisturbed environment for 5 min, followed by the collection of resting-state EEG data for 10 min. The logical principle is shown in Fig. 4A. Then, after another 5 min of rest, the subject performs MI for 10 min. During the MI session, the subject does not enter the lower limb rehabilitation robot but controls it through motor imagery. The logical principle is shown in Fig. 4B. Next, the subject enters the lower limb rehabilitation robot, rests for 5 min, and then performs MI to control the robot for 10 min. The logical principle is shown in Fig. 4C.

EEG data preprocessing

EEG data preprocessing was performed using EEGLAB v14.1.2b in MATLAB R2023b[34] (IBM Corporation, Armonk, NY, USA). The entire duration of EEG data from the first stage was retained, while for the second and third stages, only the data segments with signal strength above the activation threshold were kept. The retained data should meet the requirements for subsequent processing. The data from the three stages were grouped and named REST, MI, and MI-BCI. The following steps were performed identically for all three data groups: ① Remove the HEOR and HEOL electrooculography electrodes; ② Apply band-pass filtering (0.1–40

Hz) to eliminate unwanted frequency components and noise; ③ Manually identify and remove EEG segments contaminated by artifacts; ④ Segment the data into 2-second epochs; ⑤ Apply Independent Component Analysis (ICA) to decompose the data into independent components representing brain activity, Identify and remove components contaminated by eye movements, muscle activity, and heartbeat artifacts; ⑥ Re-reference the data to the average of all electrodes; ⑦ Manually reject periods with significant muscle artifacts or extreme amplitude values; ⑧ Retain the best continuous 90 segments (each 2 s long), resulting in a preprocessed EEG data duration of 180 s.

Microstate and brain network analysis

Microstate analysis

Before conducting microstate analysis using Cartool, the preprocessed EEG data from the three groups were further band-pass filtered in the 2–20 Hz frequency range[35]. The microstate analysis process involves several key steps:

1) Global Field Power (GFP) Calculation: Calculate the Global Field Power (GFP) to assess the brain's instantaneous electric field strength. GFP is an indicator of the brain's response to events or changes in brain activity[36]. The formula for calculating GFP is as follows:

$$GFP = \sqrt{\left(\sum_{i}^{K}\left(V_i\left(t\right) - V_{\text{mean}}\ \left(t\right)\right)^2\right)/K}$$

Where K represents the number of electrodes in the EEG data, Vi(t) represents the potential of the ith electrode at a specific time point, and Vmean(t) represents the mean instantaneous potential of all electrodes. The formula is as follows:

$$V_{\text{mean}}\ \left(t\right) = \left(\sum_{i}^{K} V_i\left(t\right)\right)/K$$

2) Topographical Mapping: In microstate analysis, the discrete states of the EEG are represented by topographical maps showing the local maxima of GFP. These local maxima of GFP are then subjected to clustering analysis to categorize all topographical maps into several types.

3) Microstate Clustering: The k-means method is initially used to divide the EEG samples into a fixed number of clusters, iteratively re-evaluating the EEG samples until the optimal cluster assignment is achieved. In this study, the clustering results identified four microstates: MS A, MS B, MS C, and MS D. The classification of four microstates is primarily determined by differences in topological structure, A: right-frontal to left-posterior; B: left-frontal to right-posterior; C: frontal to occipital; D: mostly frontal and medial to slightly less occipital activity than class C, ignoring topographic polarity[37].

4) Calculation of Microstate Parameters: After clustering the microstate topographical maps, the microstate parameters for all subjects are calculated. These parameters include Global Explained Variance (GEV), Duration, Coverage, and Occurrence.

Brain network analysis

When using the HERMES toolboxto calculate brain networks, the frequency bands are divided into δ band (0.1–4 Hz), θ band (4–8 Hz), α1 band (8–10 Hz), α2 band (10–12 Hz), β band (12–30 Hz), and γ band (30–40 Hz), and the weighted Phase Lag Index (wPLI) index is applied to eliminate volume conduction effects. A threshold is set at one standard deviation above the median connection strength, and connections below this threshold are set to 0, while those above are retained, converting the fully connected brain functional matrix into a weighted threshold network[38].

Network-based statistic (NBS) is a method specifically used for statistical analysis of brain networks or FC matrices[39]. The NBS toolbox is employed to identify subnetworks with statistically significant differences between the three groups through pairwise comparisons of brain networks under different microstates. The number of random permutations is set to 5000, and the P-value for family-wise error rate (FWER) correction is set at 0.05. The maximum subnetwork value at the 90 th percentile of the empirical distribution is denoted as S. If the size of certain subnetworks exceeds S, it indicates that these subnetworks have undergone multiple comparison corrections and show statistical differences.

Statistical analysis

The MS-Template-Explorer was used to compare the topological structures of the four microstates in the REST, MI, and MI-BCI groups, respectively[40]. SPSS 26.0 (IBM Corporation, Armonk, NY, USA) software was used for statistical analysis of the microstate time parameter data and microstate transition probabilities. To assess the significance of differences in microstate parameters across the four paradigms, an analysis of variance (ANOVA) was performed on the microstate time series parameters of all subjects. Before conducting the ANOVA, the Shapiro-Wilk test was used to assess normality. If normality is not met, the non-parametric independent-sample Kruskal-Wallis test will be used. Additionally, to control for the risk of Type I errors due to multiple comparisons, Bonferroni correction is applied for post-hoc multiple comparisons to detect differences between any two paradigms, with $P < 0.05$ considered statistically significant. The comparison of the three groups' brain networks under the four microstates was conducted using the NBS toolbox, and the results were corrected for multiple comparisons.

Results

Comparison of microstate topological structures

The similarity results of the four microstate templates in the REST, MI, and MI-BCI groups are shown in Fig. 5,which demonstrate some differences in the topological structures of the same type of microstate maps among different groups. Different colors and shades represent the polarity and magnitude of the voltage recorded by the electrodes, ignoring the polarity of the electrode maps.

Comparison of microstate time parameters

In terms of GEV values, the GEV value for REST is 0.7274, for MI it is 0.7309, and for MI-BCI it is 0.7300, which is consistent with other studies[41]. Compared with the REST paradigm, the MI and MI-BCI paradigms show an increase in the average duration and coverage of microstate D, a decrease in frequency, and a reduction in the coverage and frequency of microstate A. Compared with the MI paradigm, under the MI-BCI paradigm, the average duration of microstate C decreases, while the frequency of microstate B significantly increases. See Table 1. The transition probability results indicate that the REST paradigm has a higher transition probability towards microstate A, while the MI and MI-BCI paradigms have higher transition probabilities towards microstate D. See Table 2. The parameter results of EEG microstate can be found in Supplementary file 1.

Comparison of brain networks

Figure 6A shows the electrode connections where MI-BCI connectivity strength is greater than REST in the 0.1–4 Hz frequency band (FP1-CPz, CZ-CPz, CPz-TP7, FP1-OZ). Figure 6B shows the electrode connections where MI connectivity strength is greater than REST in the same frequency band (FC3-FC4, FC3-C3, FC4-T6, FC3-OZ, FC4-O1). Figure 6C displays the electrode connections where MI-BCI connectivity strength is greater than MI in the 4–8 Hz frequency band (Cz-P3, FT8-OZ, Cz-OZ). Figure 6D shows the electrode connections where MI-BCI connectivity strength is greater than REST in the 4–8 Hz frequency band (Fz-FC4, FC4-C4, FT8-C4, C3-C4, C3-TP7, C4-TP7). Figure 6E illustrates the electrode connections where REST connectivity strength is greater than MI-BCI in the 4–8 Hz frequency band (FP1-Cz, F7-Cz, F7-TP8, CPz-TP8, Cz-O1). Figure 6F shows the electrode connections where MI-BCI connectivity strength is greater than REST in the 8–10 Hz frequency band (F4-T4, FP1-CPz, F7-CPz, T4-CPz, F4 - T6, CPz-T6, P4-T6). Figure 6G highlights the electrode connections where MI-BCI connectivity strength is greater than MI in the 12–30 Hz frequency band (FC4-Cz, FC4-T6, Cz-O1). Figure 6H shows the electrode connections where MI-BCI connectivity strength is greater than REST in the 30–40 Hz frequency band (F4-FT7, F4-P3, F7-P3). Finally, Fig. 6I shows the electrode connections where MI connectivity strength is greater than REST in the 30–40 Hz frequency band (F4-P3, FT8-P3, FT8-T6).

Discussion

This study aimed to investigate the differences in brain activity of children with CP under REST, MI, and MI-BCI using EEG microstate and FC analysis methods. The results show that compared with REST, the differences under MI and MI-BCI are mainly between MS A and MS D; Compared with MI, the average duration of MS C

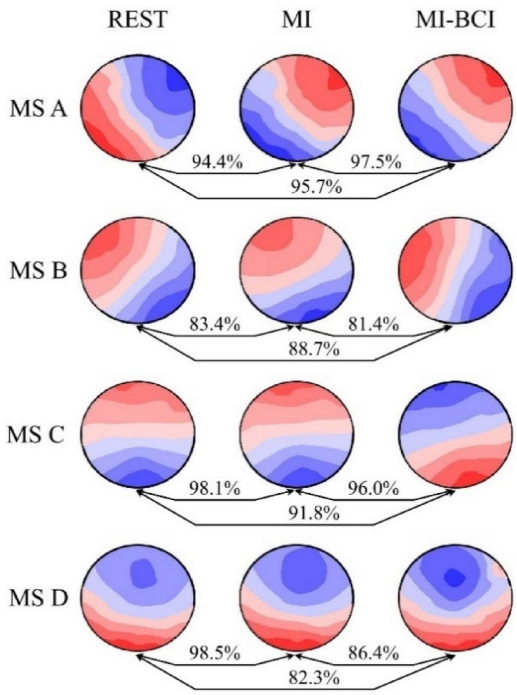

Fig. 5. The Similarity of Topological Structures of Four Microstates under REST, MI, and MI-BCI Paradigms.

Microstate parameters	Microstate categories	REST	MI	MI-BCI	Group effect	Post - hoc comparisons - *P* value			
		M (P25,P75)	M (P25,P75)	M (P25,P75)	H	P	REST vs. MI*	REST vs. MI-BCI*	MI vs. MI-BCI*
Duration (ms)	A	77.24 (71.68, 80.82)	71.98 (67.83, 77.64)	79.43 (71.75, 85.93)	4.504	0.105			
	B	76.28 (70.25, 79.17)	69.75 (66.14, 74.10)	74.47 (66.18, 82.90)	5.977	0.05			
	C	76.58 (71.71, 80.64)	80.20 (74.74, 86.13)	72.74 (68.89, 77.37)	12.282	**0.002**	0.206	0.277	**0.001**
	D	77.02 (69.76, 81.68)	82.78 (78.86, 86.13)	86.79 (79.27, 91.17)	12.741	**0.002**	**0.023**	**0.003**	> 0.99
Occurrence (hz)	A	3.36 (3.03, 3.51)	2.81 (2.55, 2.98)	2.46 (2.10, 3.30)	17.289	**< 0.001**	**0.001**	**0.004**	> 0.99
	B	3.49 (3.22, 3.58)	3.73 (3.61, 4.12)	3.59 (3.08, 3.18)	12.714	**0.002**	**0.001**	0.114	0.42
	C	3.55 (3.05, 3.62)	3.12 (2.89, 3.24)	3.35 (2.98, 3.71)	6.059	**0.048#**	0.064	> 0.99	0.168
	D	3.22 (2.79, 3.59)	3.42 (3.21, 3.75)	3.56 (3.25, 3.68)	2.901	0.234			
Coverage (%)	A	24.30 (22.06, 28.93)	21.05 (17.35, 23.39)	19.96 (15.79, 26.29)	8.157	**0.017**	**0.035**	**0.047**	> 0.99
	B	25.36 (22.83, 27.86)	26.90 (24.25, 28.66)	26.78 (23.18, 30.70)	1.871	0.391			
	C	25.77 (22.63, 28.85)	23.36 (20.99, 27.21)	24.51 (20.42, 25.81)	1.670	0.434			
	D	23.84 (20.12, 28.85)	27.82 (27.01, 29.76)	28.70 (25.91, 32.51)	10.193	**0.006**	**0.025**	**0.012**	> 0.99

Table 1. Comparison of microstate parameters among the three groups. * adjusted P-value; # close to 0.05, considered not statistically significant.

From	To	REST	MI	MI-BCI	Group effect	Post-hoc comparisons-Pvalue			
		M (P25, P75)	M (P25, P75)	M (P25, P75)	H	P	REST vs. MI*	REST vs. MI-BCI*	MI vs. MI-BCI*
A	B	0.0056 (– 0.00025, 0.0076)	0.0053 (– 0.0016, 0.0093)	0.0013 (– 0.015, 0.0079)	2.981	0.225			
A	C	– 0.0089 (– 0.012, – 0.0048)	– 0.0083 (– 0.017, 0.087)	– 0.0058 (– 0.017, 0.028)	0.413	0.813			
A	D	0.0049 (– 0.0020, 0.010)	– 0.014 (– 0.010, – 0.0033)	0.0044 (– 0.0098, 0.010)	3.897	0.142			
B	A	0.032 (0.027, 0.035)	0.027 (0.020, 0.040)	0.019 (0.010, 0.042)	5.221	0.073			
B	C	– 0.027 (– 0.035, – 0.024)	– 0.037 (– 0.040, – 0.033)	– 0.030 (– 0.042, – 0.023)	5.119	0.077			
B	D	– 0.024 (– 0.0052, – 0.0023)	0.0072 (0.0015, 0.014)	0.010 (0.00085, 0.016)	17.745	**< 0.001**	**0.004**	**< 0.001**	> 0.999
C	A	0.015 (0.010, 0.019)	0.0047(– 0.0093, 0.012)	– 0.0064(– 0.010, – 0.0016)	30.766	**< 0.001**	**0.002**	**< 0.001**	0.125
C	B	– 0.028 (– 0.035, – 0.025)	– 0.026(– 0.030, – 0.022)	– 0.024(– 0.033, – 0.021)	1.905	0.386			
C	D	0.016 (– 0.010, 0.018)	0.022 (0.014, 0.038)	0.030 (0.022, 0.047)	23.798	**< 0.001**	**0.010**	**< 0.001**	0.165
D	A	0.0055 (– 0.0073, 0.0093)	– 0.0099 (– 0.019, – 0.0019)	– 0.0023 (– 0.0059, 0.0041)	12.607	**0.002**	**0.002**	0.796	0.054
D	B	– 0.067 (– 0.011, 0.0001)	– 0.00008 (– 0.0067, 0.0049)	0.0023 (– 0.0043, 0.019)	7.694	**0.021**	0.211	**0.019**	> 0.999
D	C	– 0.0019 (– 0.0084, 0.015)	0.013 (0.001, 0.021)	– 0.0020 (– 0.011, 0.036)	9.329	**0.009**	0.202	0.686	**0.007**

Table 2. Comparison of microstate transition probabilities. * adjusted P-value.

under MI-BCI is reduced. The tendencies of microstate transition probabilities of REST, MI, and MI-BCI are not entirely the same. No FC differences were observed in the α2 band among REST, MI, and MI-BCI. In the δ and γ bands, MI and MI-BCI show stronger inter-electrode connections than REST. In the θ band, REST has stronger connections than MI-BCI, MI-BCI is stronger than REST, and MI-BCI is stronger than MI. In the α1 band, MI-BCI shows stronger connections than REST, and in the β band, MI-BCI shows stronger connections than MI.

EEG microstates

EEG microstates represent large-scale cortical neuronal activity of the cerebral cortex[42]. Each microstate is associated with a specific brain functional network. For example, Britz et al.[37]found that the four EEG microstates can be associated with the auditory network, visual network, salience network, and attention network, respectively. Previous research[43] indicates that male adolescents with mild spastic diplegia exhibit distinct EEG microstate characteristics compared to healthy individuals, including an increased occurrence of microstate classes A and D and a reduced duration of microstate class B. These differences support an understanding of the neurofunctional specificities in children with CP.

In this study, the duration and coverage of microstate D significantly increased under MI and MI-BCI compared to REST, suggesting that these conditions alter EEG activity patterns. Microstate D, associated with the dorsal attention network, reflects attention and focus shifts. Under MI and MI-BCI, subjects require heightened attention, increasing microstate D's time parameters, likely activating motor-related areas such as the motor and premotor cortex. Meanwhile, the average duration and coverage of microstate A decreased. Microstate A is believed to be associated with lower sensory areas[44], which are more active in the resting state. This may

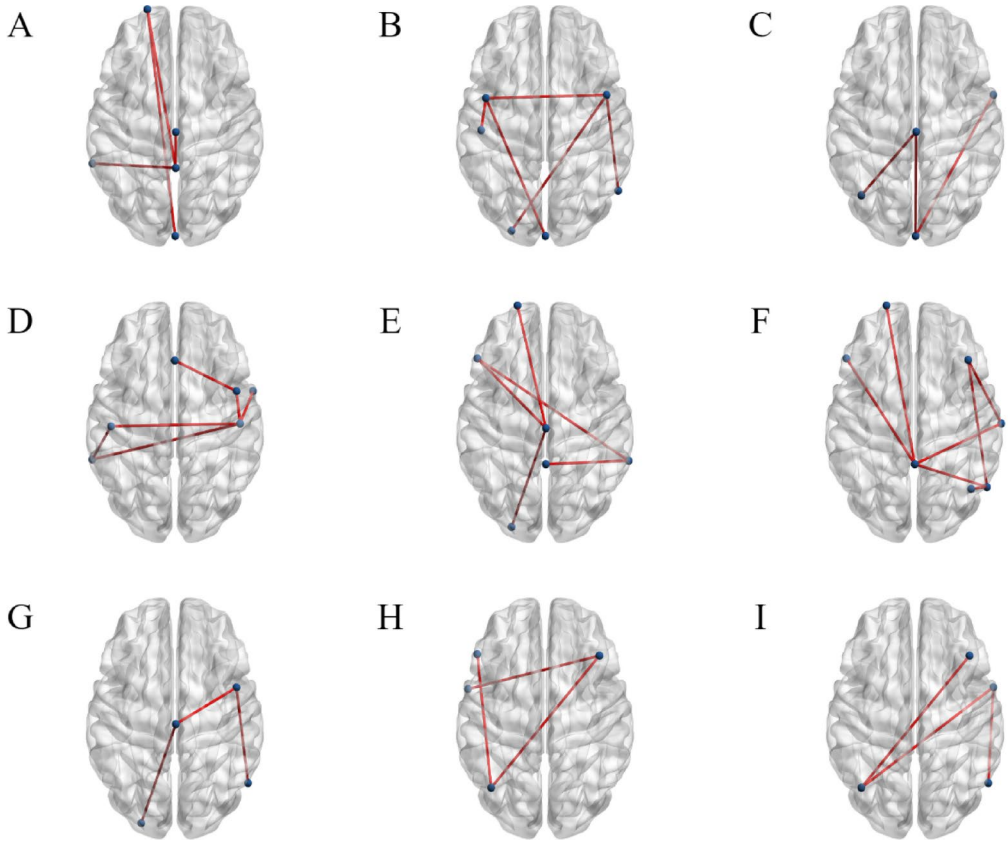

Fig. 6. Comparison of brain network connection strength differences. (**A**) 0.1–4 Hz, MI-BCI > REST; (**B**) 0.1–4 Hz, MI > REST; (**C**) 4–8 Hz, MI-BCI > MI; (**D**) 4–8 Hz, MI-BCI > REST; (**E**) 4–8 Hz, REST > MI-BCI; (**F**) 8–10 Hz, MI-BCI > REST; (**G**) 12–30 Hz, MI-BCI > MI; (**H**) 30–40 Hz, MI-BCI > REST; (**I**) 30–40 Hz, MI > REST.

be related to the need for higher cognitive attention in children under MI. Compared with MI, the average duration of microstate C in children under MI-BCI decreased. This is consistent with studies on microstate changes during cognitive tasks such as mental arithmetic tasks[45]. Microstate C reflects a part of the default mode network. The default mode network is a task-negative network, and its activity decreases during the execution of cognitive tasks. Compared to MI, MI-BCI more effectively enhances brain involvement and boosts children's participation in physical training, likely due to increased active engagement. The frequency of microstate B also rose, possibly reflecting the brain's response to motor feedback from the rehabilitation robot, activating areas related to arousal regulation and cognitive control.

The research indicates that microstate transitions are non-random and require further investigation to connect these transition probabilities with functional networks[36]. This study found higher transition probabilities to microstate A in children with CP during REST. While it did not analyze speech related to microstate A, previous research has shown reduced speech function in these children[46]. Under MI and MI-BCI, transition probabilities to microstate D were higher, likely reflecting children's active participation. This dynamic transition shows how the brain adapts its functional state in children with CP to better manage cognitive and motor tasks during motor imagery and robot interaction.

EEG brain functional networks

Brain functional activities can be studied through network neuroscience by measuring correlations between brain regions to identify connections of varying strengths[47]. The brain's electrophysiological activities are divided into frequency bands, each with distinct scalp distribution and biological significance[48].

In the δ band, MI-BCI task connection strength is notably higher than REST, especially between FP1-CPz, CZ-CPz, CPz-TP7, and FP1-OZ electrodes. The prefrontal area (FP1) is key in attention and cognitive control[49], while the central area (CPz) and occipital area (OZ) are related to motor control and visual processing[50]. This enhanced connection may reflect the need for higher attention and cognitive control to complete complex tasks in BCI tasks. Low-frequency EEG activity is usually associated with motor preparation[51], indicating that in this state, BCI tasks may trigger higher cognitive load and mental concentration.Similarly, in the δ frequency band, the connection strength under the MI task state is higher than in the REST state, particularly between the FC3-FC4, FC3-C3, FC4-T6, FC3-OZ, and FC4-O1 electrodes. The FC3 and FC4 electrodes are located in the frontal motor area, involved in motor planning and execution[52]. This enhanced connection may reflect the brain's high demand for motor-related areas during motor imagery, as it simulates movement without limb motion, aligning

with increased low-frequency EEG activity and indicating high brain integration during introspection and imagery.

In the θ band, MI-BCI task connection strength is significantly higher than MI, particularly between Cz-P3, FT8-OZ, and Cz-OZ electrodes. Enhanced connections among central (Cz), parietal (P3), and occipital (OZ) areas suggest closer cooperation in BCI tasks, likely related to the visuomotor integration needed for task execution[53]. EEG activity in this frequency band (θ waves) is usually associated with memory and learning[54], indicating that BCI tasks may enhance connections in brain regions related to cognition and memory. In the same frequency band, MI-BCI task connection strength surpasses REST, notably between Fz-FC4, FC4-C4, FT8-C4, C3-C4, C3-TP7, and C4-TP7 electrodes. These prefrontal, frontal, and parietal areas demand stronger connections during task execution, reflecting extensive information processing and high cooperation among brain regions in BCI tasks.

In the α1 band, MI-BCI task connection strength is significantly higher than REST, especially between F4-T4, FP1-CPz, F7-CPz, T4-CPz, F4 -T6, CPz-T6, and P4-T6 electrodes. Enhanced connections among prefrontal, parietal, and temporal regions suggest closer cooperation for information processing and task execution in BCI tasks. Mid-frequency α waves typically relate to relaxation and eyes-closed rest, but their increased activity during BCI tasks suggests alertness and cognitive load. No differences were observed in the α2 band across the three conditions.

In the β band, MI-BCI task connection strength is significantly higher than MI, particularly between FC4-Cz, FC4-T6, and Cz-O1 electrodes. Enhanced connections among FC4, Cz, and O1 likely reflect motor control and visual processing demands in these regions[55]. High-frequency β waves, typically linked to active thinking, anxiety, and focus, indicate a high demand for brain region integration during BCI tasks.

In the γ band, MI-BCI task connection strength is significantly higher than REST, especially between F4-FT7, F4-P3, and F7-P3 electrodes. Enhanced prefrontal-temporal connections suggest greater brain activity and synchrony demands in the ultra-high frequency band during BCI tasks. High γ band activity has also been observed during treadmill walking[56]. This suggests that enhanced connections in this frequency band during BCI tasks may reflect the brain's efficient integration for complex tasks.

These results show significant differences in brain network connections across frequency bands between MI-BCI, MI, and REST states. MI-BCI tasks demonstrate higher connection strength, indicating greater brain region coordination needs. Connection variations in prefrontal, parietal, occipital, and temporal areas highlight their roles in cognitive and motor tasks, providing a theoretical basis to advance brain-computer interface research and optimize related technologies.

Limitations and prospects

The experiment had a small sample size of 20 cases and did not include long-term rehabilitation to assess efficacy. Due to equipment and participant cooperation limitations, the paradigm in Fig. 4B was used to collect EEG data for the MI paradigm. Research indicates that children with CP can perform MI but with increased errors[57]. The MI performance of children with CP is affected by functional ability and memory. During EEG collection, they often display frequent, uncontrolled movements, potentially causing motion artifacts. This study analyzed only the temporal properties of four EEG microstates and the spatial properties of EEG FC. Future research could explore multidimensional EEG characteristics, such as frequency domain analysis, ERD, and EEG source activity, to deepen understanding of MI and MI-BCI effects on brain activity in children with CP.

Conclusion

This study, using EEG microstate and FC analysis, shows that MI-BCI significantly alters brain activity patterns in children with CP, enhancing attention, motor planning, execution, and FC strength across frequency bands. These findings confirm MI-BCI's substantial application value in lower limb motor rehabilitation for children with CP.

Data availability

The raw EEG data that support the findings of this study are available on request from the corresponding author.

Received: 19 September 2024; Accepted: 1 April 2025
Published online: 10 April 2025

References

1. Paul, S., Nahar, A., Bhagawati, M. & Kunwar, A. J. A Review on Recent Advances of Cerebral Palsy. *Oxid. Med. Cell. Longev.* 2622310 (2022). (2022).
2. Vitrikas, K., Dalton, H. & Breish, D. Cerebral palsy: an overview. *Am. Fam Physician*. **101**, 213–220 (2020).
3. Chen, Y. P. & Howard, A. M. Effects of robotic therapy on upper-extremity function in children with cerebral palsy: A systematic review. *Dev. Neurorehabilitation*. **19**, 64–71 (2016).
4. Fandim, J. V., Saragiotto, B. T., Porfírio, G. J. M. & Santana, R. F. Effectiveness of virtual reality in children and young adults with cerebral palsy: a systematic review of randomized controlled trial. *Braz J. Phys. Ther.* **25**, 369–386 (2021).
5. Pichiorri, F. & Mattia, D. Brain-computer interfaces in neurologic rehabilitation practice. *Handb. Clin. Neurol.* **168**, 101–116 (2020).
6. Rimbert, S. & Fleck, S. Long-term kinesthetic motor imagery practice with a BCI: impacts on user experience, motor cortex oscillations and BCI performances. *Comput. Hum. Behav.* **146**, 107789 (2023).
7. Mane, R., Chouhan, T. & Guan, C. BCI for stroke rehabilitation: motor and beyond. *J. Neural Eng.* **17**, 041001 (2020).
8. Wang, Z. et al. Enhancing ERD activation and functional connectivity via the Sixth-finger motor imagery in stroke patients. *IEEE Trans. Neural Syst. Rehabil Eng. Publ IEEE Eng. Med. Biol. Soc.* PP, (2024).
9. Williams, J., Reid, S. M., Reddihough, D. S. & Anderson, V. Motor imagery ability in children with congenital hemiplegia: effect of lesion side and functional level. *Res. Dev. Disabil.* **32**, 740–748 (2011).

10. Gentile, A. E. et al. Motor imagery for paediatric neurorehabilitation: how much do we know? Perspectives from a systematic review. *Front. Hum. Neurosci.* **18**, 1245707 (2024).
11. Grèzes, J. & Decety, J. Functional anatomy of execution, mental simulation, observation, and verb generation of actions: a meta-analysis. *Hum. Brain Mapp.* **12**, 1–19 (2001).
12. Kuo, H. C. et al. Using diffusion tensor imaging to identify corticospinal tract projection patterns in children with unilateral spastic cerebral palsy. *Dev. Med. Child. Neurol.* **59**, 65–71 (2017).
13. Neuper, C., Scherer, R., Reiner, M. & Pfurtscheller, G. Imagery of motor actions: differential effects of kinesthetic and visual-motor mode of imagery in single-trial EEG. *Brain Res. Cogn. Brain Res.* **25**, 668–677 (2005).
14. Gözaçan Karabulut, D., Tütün Yümin, E. & Öztürk, Y. The effect of motor imagery training on individuals with unilateral cerebral palsy on motor imagery ability, functional mobility and muscle activity. *Somatosens Mot Res.* **39**, 62–69 (2022).
15. Hétu, S. et al. The neural network of motor imagery: an ALE meta-analysis. *Neurosci. Biobehav Rev.* **37**, 930–949 (2013).
16. Yuanqing et al. Multimodal BCIs: Target Detection, Multidimensional Control, and Awareness Evaluation in Patients With Disorder of Consciousness. *Proc. IEEE* 104, 332–352 (2016).
17. Behboodi, A., Lee, W. A., Hinchberger, V. S. & Damiano, D. L. Determining optimal mobile neurofeedback methods for motor neurorehabilitation in children and adults with non-progressive neurological disorders: a scoping review. *J. Neuroeng. Rehabil.* **19**, 104 (2022).
18. Qu, H. et al. The clinical effects of brain-computer interface with robot on upper-limb function for post-stroke rehabilitation: a meta-analysis and systematic review. *Disabil. Rehabil Assist. Technol.* **19**, 30–41 (2024).
19. Mokienko, O. A. et al. Increased motor cortex excitability during motor imagery in brain-computer interface trained subjects. *Front. Comput. Neurosci.* **7**, 168 (2013).
20. Behboodi, A. et al. Development and evaluation of a BCI-neurofeedback system with real-time EEG detection and electrical stimulation assistance during motor attempt for neurorehabilitation of children with cerebral palsy. *Front. Hum. Neurosci.* **18**, 1346050 (2024).
21. Xie, J. et al. Rehabilitation of motor function in children with cerebral palsy based on motor imagery. *Cogn. Neurodyn.* **15**, 939–948 (2021).
22. Pascual-Marqui, R. D., Michel, C. M. & Lehmann, D. Segmentation of brain electrical activity into microstates: model Estimation and validation. *IEEE Trans. Biomed. Eng.* **42**, 658–665 (1995).
23. Lehmann, D. et al. EEG microstate duration and syntax in acute, medication-naive, first-episode schizophrenia: a multi-center study. *Psychiatry Res.* **138**, 141–156 (2005).
24. Ma, S., Yan, X., Billington, J., Merat, N. & Markkula, G. Cognitive load during driving: EEG microstate metrics are sensitive to task difficulty and predict safety outcomes. *Accid. Anal. Prev.* **207**, 107769 (2024).
25. Günther, W. et al. Quantitative EEG analysis during motor function and music perception in tourette's syndrome. *Eur. Arch. Psychiatry Clin. Neurosci.* **246**, 197–202 (1996).
26. Daly, I. et al. On the control of brain-computer interfaces by users with cerebral palsy. *Clin. Neurophysiol. Off J. Int. Fed. Clin. Neurophysiol.* **124**, 1787–1797 (2013).
27. Liu, W., Liu, X., Dai, R. & Tang, X. Exploring differences between left and right hand motor imagery via spatio-temporal EEG microstate. *Comput. Assist. Surg. Abingdon Engl.* **22**, 258–266 (2017).
28. Li, Y., Chen, M., Sun, S. & Huang, Z. Exploring differences for motor imagery using Teager energy operator-based EEG microstate analyses. *J. Integr. Neurosci.* **20**, 411–417 (2021).
29. Müller-Putz, G. R., Daly, I. & Kaiser, V. Motor imagery-induced EEG patterns in individuals with spinal cord injury and their impact on brain-computer interface accuracy. *J. Neural Eng.* **11**, 035011 (2014).
30. Dennis, E. L. & Thompson, P. M. Functional brain connectivity using fMRI in aging and Alzheimer's disease. *Neuropsychol. Rev.* **24**, 49–62 (2014).
31. Marchitelli, R. et al. Dynamic functional connectivity in Adolescence-Onset major depression: relationships with severity and symptom dimensions. *Biol. Psychiatry Cogn. Neurosci. Neuroimaging.* **7**, 385–396 (2022).
32. Wang, L. et al. Dynamic functional reorganization of the motor execution network after stroke. *Brain J. Neurol.* **133**, 1224–1238 (2010).
33. Yuan, Z. et al. Effect of BCI-Controlled pedaling training system with multiple modalities of feedback on motor and cognitive function rehabilitation of early subacute stroke patients. *IEEE Trans. Neural Syst. Rehabil Eng.* **29**, 2569–2577 (2021).
34. Delorme, A. & Makeig, S. EEGLAB: an open source toolbox for analysis of single-trial EEG dynamics including independent component analysis. *J. Neurosci. Methods*. **134**, 9–21 (2004).
35. Brunet, D., Murray, M. M. & Michel, C. M. Spatiotemporal Analysis of Multichannel EEG: CARTOOL. *Comput. Intell. Neurosci.* 1–15 (2011). (2011).
36. Khanna, A., Pascual-Leone, A., Michel, C. M. & Farzan, F. Microstates in resting-state EEG: current status and future directions. *Neurosci. Biobehav Rev.* **49**, 105–113 (2015).
37. Britz, J., Van De Ville, D. & Michel, C. M. BOLD correlates of EEG topography reveal rapid resting-state network dynamics. *NeuroImage* **52**, 1162–1170 (2010).
38. Mohanty, R., Sethares, W. A., Nair, V. A. & Prabhakaran, V. Rethinking measures of functional connectivity via feature extraction. *Sci. Rep.* **10**, 1298 (2020).
39. Zalesky, A., Fornito, A. & Bullmore, E. T. Network-based statistic: identifying differences in brain networks. *NeuroImage* **53**, 1197–1207 (2010).
40. Koenig, T. et al. EEG-Meta-Microstates: towards a more objective use of Resting-State EEG microstate findings across studies. *Brain Topogr*. **37**, 218–231 (2024).
41. Khanna, A., Pascual-Leone, A. & Farzan, F. Reliability of resting-state microstate features in electroencephalography. *PloS One*. **9**, e114163 (2014).
42. Michel, C. M. & Koenig, T. EEG microstates as a tool for studying the Temporal dynamics of whole-brain neuronal networks: A review. *NeuroImage* **180**, 577–593 (2018).
43. F, G. & Y, F. H, J., X, W., D, Y. Altered Resting-State EEG microstate parameters and enhanced Spatial complexity in male adolescent patients with mild spastic diplegia. *Brain Topogr* **30**, (2017).
44. Gui, P. et al. Assessing the depth of Language processing in patients with disorders of consciousness. *Nat. Neurosci.* **23**, 761–770 (2020).
45. Bréchet, L. et al. Capturing the Spatiotemporal dynamics of self-generated, task-initiated thoughts with EEG and fMRI. *NeuroImage* **194**, 82–92 (2019).
46. Nip, I. S. B. Kinematic characteristics of speaking rate in individuals with cerebral palsy: A preliminary study. *J. Med. Speech-Lang Pathol.* **20**, 88–94 (2013).
47. Bassett, D. S. & Sporns, O. Network neuroscience. *Nat. Neurosci.* **20**, 353–364 (2017).
48. Babiloni, C. et al. International federation of clinical neurophysiology (IFCN) - EEG research workgroup: recommendations on frequency and topographic analysis of resting state EEG rhythms. Part 1: applications in clinical research studies. *Clin. Neurophysiol. Off J. Int. Fed. Clin. Neurophysiol.* **131**, 285–307 (2020).
49. Nyberg, L. Cognitive control in the prefrontal cortex: A central or distributed executive? *Scand. J. Psychol.* **59**, 62–65 (2018).
50. Fattori, P., Breveglieri, R., Bosco, A., Gamberini, M. & Galletti, C. Vision for prehension in the medial parietal cortex. *Cereb. Cortex N Y N 1991*. **27**, 1149–1163 (2017).

51. Magnuson, J. R. & McNeil, C. J. Low-frequency neural activity at rest is correlated with the movement-related cortical potentials elicited during both real and imagined movements. *Neurosci. Lett.* **742**, 135530 (2021).
52. Tatti, E. et al. Frontal increase of beta modulation during the practice of a motor task is enhanced by visuomotor learning. *Sci. Rep.* **11**, 17441 (2021).
53. Hülsdünker, T., Strüder, H. K. & Mierau, A. The athletes' visuomotor system - Cortical processes contributing to faster visuomotor reactions. *Eur. J. Sport Sci.* **18**, 955–964 (2018).
54. Zielinski, M. C., Tang, W. & Jadhav, S. P. The role of replay and theta sequences in mediating hippocampal-prefrontal interactions for memory and cognition. *Hippocampus* **30**, 60–72 (2020).
55. Bottari, D. et al. Motion processing after sight restoration: no competition between visual recovery and auditory compensation. *NeuroImage* **167**, 284–296 (2018).
56. Castermans, T., Duvinage, M., Cheron, G. & Dutoit, T. About the cortical origin of the low-delta and high-gamma rhythms observed in EEG signals during treadmill walking. *Neurosci. Lett.* **561**, 166–170 (2014).
57. Souto, D. O., Cruz, T. K. F., Fontes, P. L. B. & Haase, V. G. Motor imagery in children with unilateral cerebral palsy: a case-control study. *Dev. Med. Child. Neurol.* **62**, 1396–1405 (2020).

Author contributions

D.Z. is the principle investigator and data custodian Study. Data analysis was performed by W.Q., Y.Z., Z.H., Y.S., S.L., H.W. and D.Z. The first draft of the manuscript was prepared by W.Q., Y.Z., Z.H. revised by W.Q., J.Z., K.S., M.W., L.Z. and D.Z. All authors approved the final draft of the manuscript and agreed to be accountable for all aspects of the work in ensuring that questions related to the accuracy or integrity of any part of the work are appropriately investigated and resolved.

Funding

This study was funded by the construction of precise rehabilitation management platform for disabled children based on cloud services, key research and development and promotion special project (technology breakthrough) in Henan Province in 2023, 2023.1 - 2024.12, project number: 232102310135.

Declarations

Competing interests

The authors declare no competing interests.

Ethical approval

The current study was approved by the Ethics Committee of the Third Affiliated Hospital of Zhengzhou University (No. 2023 - 184 - 01).

Additional information

Supplementary Information The online version contains supplementary material available at https://doi.org/10.1038/s41598-025-96946-z.

Correspondence and requests for materials should be addressed to D.Z.

Reprints and permissions information is available at www.nature.com/reprints.

Publisher's note Springer Nature remains neutral with regard to jurisdictional claims in published maps and institutional affiliations.